

RESEARCH

Open Access



# MiR-147b-3p promotes osteogenesis by targeting NDUFA4 and PI3K/AKT pathway

Yuanyuan Guo<sup>1,2†</sup>, Kai Shen<sup>3†</sup>, Zhijie Li<sup>2</sup>, Changchun Niu<sup>2\*</sup> and Yang Luo<sup>1,4,5\*</sup>

## Abstract

**Background** Osteoporosis (OP) is a progressive metabolic bone disease characterized by impaired bone microarchitecture, decreased bone strength, and dysregulated bone remodeling, leading to an increased risk of fractures. Among osteoporotic fractures, osteoporotic vertebral compression fractures (OVCF) are the most common and can significantly impact patients' quality of life. Growing evidence suggests that microRNAs (miRNAs) play a crucial role in bone homeostasis by regulating osteoblast differentiation, bone metabolism, and remodeling processes. Notably, miR-147b-3p has been found to be downregulated in OVCF; however, its specific role in osteogenic regulation remains largely unknown. Therefore, further investigation is warranted to elucidate the function and underlying mechanism of miR-147b-3p in osteogenic differentiation.

**Methods** The GSE93883 and GSE74209 datasets were retrieved from the Gene Expression Omnibus (GEO) database to investigate specific microRNAs involved in the regulation of osteogenesis. Differential expression of miR-147b-3p and NDUFA4 was assessed between healthy controls and patients with osteoporotic vertebral compression fractures (OVCF) using real-time quantitative PCR. To modulate the expression levels of miR-147b-3p in MC3T3-E1 cells, both the miR-147b-3p mimic and inhibitor were utilized. Cell viability was evaluated via the CCK-8 assay to assess the impact of miR-147b-3p on MC3T3-E1 cell proliferation. Real-time PCR and Western blot analysis were conducted to quantify the expression levels of osteogenic markers across different experimental groups. Alizarin red staining (ARS) was employed to examine the effect of miR-147b-3p on the mineralization capacity of MC3T3-E1 cells. In vivo experiments were performed to evaluate the functional role of miR-147b-3p. Bioinformatics databases were used to predict the potential target gene of miR-147b-3p (NDUFA4), and the predictions were validated by a dual luciferase reporter gene assay. To investigate the regulatory role of the miR-147b-3p/NDUFA4 axis in osteogenic differentiation, MC3T3-E1 cells were transfected with the NDUFA4 overexpression plasmid and miR-147b-3p mimic. Western blot analysis was performed to assess the phosphorylation levels of PI3K and AKT, in order to explore whether the miR-147b-3p/NDUFA4 axis regulates osteogenic differentiation through the PI3K/AKT signaling pathway.

**Results** Our results indicated a significant downregulation of miR-147b-3p and a concurrent upregulation of NDUFA4 in patients with osteoporotic vertebral compression fractures (OVCF). A luciferase reporter assay confirmed

<sup>†</sup>Yuanyuan Guo and Kai Shen contributed equally to this work.

\*Correspondence:  
Changchun Niu  
bright\_star2000@163.com  
Yang Luo  
luoy@cqu.edu.cn

Full list of author information is available at the end of the article



© The Author(s) 2025. **Open Access** This article is licensed under a Creative Commons Attribution-NonCommercial-NoDerivatives 4.0 International License, which permits any non-commercial use, sharing, distribution and reproduction in any medium or format, as long as you give appropriate credit to the original author(s) and the source, provide a link to the Creative Commons licence, and indicate if you modified the licensed material. You do not have permission under this licence to share adapted material derived from this article or parts of it. The images or other third party material in this article are included in the article's Creative Commons licence, unless indicated otherwise in a credit line to the material. If material is not included in the article's Creative Commons licence and your intended use is not permitted by statutory regulation or exceeds the permitted use, you will need to obtain permission directly from the copyright holder. To view a copy of this licence, visit <http://creativecommons.org/licenses/by-nc-nd/4.0/>.

that NDUFA4 is a direct target gene of miR-147b-3p. To examine the functional role of miR-147b-3p, both in vitro and in vivo experiments were conducted. The experimental findings revealed that the miR-147b-3p mimic significantly enhanced cell viability, increased protein expressions of Alkaline Phosphatase (ALP) and Runt-related Transcription Factor 2 (RUNX2), and promoted mineralization as evidenced by Alizarin Red S staining. Conversely, treatment with the miR-147b-3p inhibitor or overexpression plasmid for NDUFA4 (pNDUFA4) produced opposite effects. Furthermore, the miR-147b-3p/NDUFA4 axis was found to regulate the PI3K/AKT signaling pathway. The miR-147b-3p mimic significantly increased the phosphorylation levels of PI3K (p-PI3K) and AKT (p-AKT), whereas pNDUFA4 led to their reduction.

**Conclusions** This study demonstrated that miR-147b-3p plays a crucial role in promoting osteogenic differentiation in osteoporotic vertebral compression fractures (OVCF) by targeting NDUFA4 and modulating the PI3K/AKT signaling pathway. These findings provide new insights into the molecular mechanisms underlying the progression of osteoporotic vertebral fractures.

**Keywords** MiR-147b-3p, Type I coenzyme dehydrogenase 1 $\alpha$  subcomplex 4 (NDUFA4), Phosphatidylinositol 3-kinase (PI3K)/AKT pathway, Osteogenesis vertebral compression fractures (OVCF)

## Introduction

As numerous countries worldwide, particularly those in Asia, progressively transition into an aging society, the incidence of osteoporosis (OP) and its associated complications inevitably rise. Among these complications, osteoporotic vertebral compression fractures (OVCF) stand out as the most prevalent [1, 2]. Osteogenesis represents a complex dynamic genetic modification program within osteoblasts that culminates in the synthesis of a collagen mineralized matrix and plays a pivotal role in maintaining bone homeostasis [3]. The regulation of bone formation by osteoblast lineage cells involves intricate mechanisms encompassing both genetic and epigenetic control, including histone modification, DNA methylation, and chromatin structure [4]. In addition, microRNAs (miRNAs) also exert post-transcriptional epigenetic regulation on osteogenesis through their targeting of mRNA molecules related to osteoblast function [5].

MicroRNAs (miRNAs) are small, single-stranded, non-coding RNAs with an average length of 22 nucleotides. They exert their biological functions by down-regulating gene expression through translation inhibition or mRNA target degradation [6, 7]. Numerous studies have demonstrated the involvement of miRNAs in various biological processes, including apoptosis, cancer development, osteoblast formation, and osteoclastogenesis [8–10]. Furthermore, emerging evidence suggests that miRNAs may play a significant role in the pathogenesis of bone diseases [11, 12]. For instance, Ze Long et al. reported that miR-181a-5p promotes osteogenesis by targeting BMP3 [13]. Ding Li et al. illustrated the miR-4739/DLX3 axis regulates the differentiation ability of bone marrow mesenchymal stem cells into osteoblasts and potentially contributes to the pathogenesis of osteoporosis [14]. Fujiang Zhao et al. demonstrated that miR-483-5p is implicated in postmenopausal osteoporosis by inhibiting SATB2 and

activating the PI3K/AKT pathway, indicating its potential as a therapeutic target for intervention [15]. However, the role of miR-147b-3p in relation to osteoporosis and vertebral compression fractures remains unclear.

Thus, this study aimed to investigate the expression of miR-147b-3p in individuals with osteoporotic vertebral compression fractures following screening for miRNAs with varying expression from a Gene Expression Omnibus (GEO) dataset. Furthermore, the effects of miR-147b-3p on bone formation and resorption were assessed. Subsequently, the target gene of miR-147b-3p was identified through luciferase reporter assays. Additionally, MC3T3-E1 cells were utilized to explore the role and mechanism of miR-147b-3p in osteogenic differentiation.

## Materials and methods

### Bioinformatic analysis

The GSE93883 and GSE74209 datasets were obtained from the Gene Expression Omnibus (GEO) database (<https://www.ncbi.nlm.nih.gov/geo/>). Target mRNAs of microRNAs were predicted using TargetScan (<https://www.targetscan.org/>), miRWalk (<http://mirwalk.umm.uni-heidelberg.de/>), and miRDB (<http://mirdb.org/>). Differentially expressed microRNAs between osteoporotic vertebral compression fracture (OVCF) samples and healthy controls were identified using the GEO2R online analysis tool (<https://www.ncbi.nlm.nih.gov/geo/geo2r/>). Gene Ontology (GO) annotation and Kyoto Encyclopedia of Genes and Genomes (KEGG) pathway enrichment analyses were performed using the Metascape online database (<http://metascape.org>).

### Sample collection

A total of 30 patients diagnosed with osteoporotic vertebral fractures at the Spinal Surgery Department of Chongqing General Hospital between June 2021 and

December 2022 were recruited for this study. An additional cohort of 30 healthy individuals was included as the control group during the same period. Bone mineral density (BMD) classification was based on the World Health Organization (WHO) criteria. A T-score greater than  $-1.0$  was considered normal, while osteopenia was defined as a T-score between  $-1.0$  and  $-2.5$ , indicating reduced bone density without meeting the threshold for osteoporosis. Osteoporosis was diagnosed in individuals with a T-score of  $-2.5$  or lower, whereas severe or established osteoporosis was characterized by a T-score of  $-2.5$  or lower accompanied by one or more osteoporotic fractures.

Patients in the OVCF group were required to exhibit clinical symptoms such as localized low back pain, spinal deformity, or neurological impairment, along with a confirmed imaging diagnosis and a BMD T-score  $\leq -2.5$  standard deviations (SD). Exclusion criteria included severe hepatic or renal dysfunction, coagulation disorders, arthritis, systemic immune diseases, and long-term use of medications known to affect bone metabolism.

#### Cell culture and treatment

MC3T3-E1 cells were obtained from the Chinese Academy of Sciences Cell Library (China, originally sourced from ATCC, USA). The cells were cultured in  $\alpha$ -modified minimal essential medium ( $\alpha$ -MEM) supplemented with 10% fetal bovine serum (FBS) (Pricella Biotechnology Co., Ltd., Wuhan, China), 50 mg/mL streptomycin, and 50 IU/mL penicillin. The cultures were maintained in a humidified incubator at 37 °C with 5% CO<sub>2</sub>. To induce osteogenic differentiation, the medium was further supplemented with 100 nM dexamethasone, 10 mM  $\beta$ -glycerophosphate sodium, and 50 mg/L ascorbic acid.

miR-147b-3p inhibitors and mimics were purchased from RiboBio Co., Ltd. (Guangzhou, China), and transfection was performed using Lipofectamine 6000 (Beyotime Co., Ltd., Shanghai, China) according to the manufacturer's instructions.

#### Cell counting kit-8 (CCK-8) assay for cell viability

Cells subjected to treatment or transfection were seeded into 24-well plates at a density of  $1 \times 10^4$  cells per well. After incubation, 10  $\mu$ L of CCK-8 solution (Beyotime Co., Ltd., Shanghai, China) was added to each well, followed by further incubation at 37 °C for 3 h. The optical density (OD) at 450 nm was then measured using a microplate reader to assess cell viability.

#### Alizarin red S (ARS) staining

Mineral nodule formation was assessed using the Alizarin Red S (ARS) Kit (Beyotime, China). According to the manufacturer's instructions, cells were fixed with 4% paraformaldehyde for 20 min, followed by staining with

ARS staining reagent for 30 min. The cells were then washed with the provided buffer and observed under an inverted microscope.

#### Mice and treatment

C57BL/6J wild-type mice aged 6 months and 18 months were obtained from Chang Zhou Cavens Model Animal Co., Ltd. (Jiangsu, China). The 18-month-old mice were administered antagomir-miR-147b-3p or antagomir-negative control (10 mg/kg body weight) using an osteoblast-targeted delivery system via tail vein injection twice per week for four weeks [16].

#### Micro-CT analysis

Tibias were scanned using a micro-CT system (Sky-scan, Bruker) at a scanning resolution of 18  $\mu$ m. Three-dimensional (3D) reconstruction of trabecular bone was performed using CTVol software. The following bone parameters were analyzed: bone surface density (BS/TV), bone volume fraction (BV/TV), trabecular separation (Tb.Sp), trabecular number (Tb.N), trabecular pattern factor (Tb.Pf), and trabecular thickness (Tb.Th) [16, 17].

#### Dual-luciferase reporter assay

Potential miR-147b-3p target genes were predicted using TargetScan 7.1 software (<http://www.targetscan.org/>). The wild-type (WT) and mutant (MUT) 3'-UTR sequences of NDUFA4 were cloned into dual-luciferase reporter vectors (Promega, USA). The reporter vectors were co-transfected with miR-147b-3p mimics, inhibitors, or negative controls (NC) into 293T cells. After 48 h of transfection, luciferase activity was measured using a dual-luciferase reporter assay kit (Promega, USA). Each experiment was performed in triplicate.

#### Real-time quantitative PCR (RT-qPCR)

Total RNA was extracted from target cells and blood samples using nucleic acid extraction and purification kits (Zybio, China). Reverse transcription of total RNA was performed using a PrimeScript RT kit (Takara Bio, Shiga, Japan). RT-qPCR was conducted on an ABI Prism 7500 Sequence Detection System (Applied Biosystems, USA) using the TB Green<sup>®</sup> Premix Ex Taq<sup>™</sup> II Kit (Takara Bio, Shiga, Japan). U6 and GAPDH were used as internal references for miRNA and mRNA quantification, respectively. Relative expression levels were calculated using the  $2^{-\Delta\Delta CT}$  method. All experiments were performed in triplicate. The primer sequences were: miR-147b-3p, forward, 5'-CGGTGTGCGGAAATGCT-3' and reverse, 5'-AGTGCAGGGTCCGAGGTATT-3'; U6, forward, 5'-CTCGCTTCGGCAGCAC-3' and reverse, 5'-AACGCTTCACGAATTTGCG-3'; NDUFA4, forward, 5'-CCCTCTTTGTATTTATTGG-3' and

reverse, 5'-GCTCTGGGTTATTTCTGTC-3; GAPDH,

forward, 5'-GGAGAGTGTTCCTCGTCCC-3' and reverse, 5'-ACTGTGCCGTTGAATTTGCC-3'.

#### Western blot assay

The RIPA buffer containing protease inhibitors (Beyotime, Shanghai, China) was utilized for protein sample extraction from target cells. The BCA quantitative method (Beyotime) was employed to determine the concentration of the protein samples. SDS-PAGE (10%) was utilized to separate the collected protein samples, which were subsequently transferred onto PVDF membranes (Millipore, Burlington, MA, USA). A non-fat milk (5%) solution was used for membrane incubation for 2 h to prevent non-specific binding. The following antibodies were applied for overnight incubation at 4 °C: ALP (1:1000, HuaBio), RUNX2 (1:1000, HuaBio), AKT1/23 (1:1000, HuaBio), PI3Kp85 (1:1000, HuaBio), phospho-AKT1 (1:1000, HuaBio), phospho-PI3Kp85 (1:1000, HuaBio), NDUFA4 (1:1000, HuaBio). Subsequently, appropriate secondary antibodies (HuaBio; 1:5000) were used for membrane incubation at room temperature for 2 h after primary antibody incubation. Enhanced Chemiluminescence Fluorescence Detection Kit (ECL; Beyotime, Shanghai, China) was employed to visualize the blot signal on a Bio-Rad image analysis system (Bio-Rad, Hercules, CA, USA). The relative protein content is expressed as the gray value of the corresponding protein band/GAPDH protein band.

#### Statistical analysis

Statistical analyses were conducted using GraphPad Prism 8.0 software. Data are presented as mean  $\pm$  standard deviation (SD). Each experiment was performed in triplicate to minimize systematic and random errors. For comparisons between two groups, an unpaired Student's t-test was applied. For multiple group comparisons, one-way analysis of variance (ANOVA) followed by Tukey's post hoc test was used. P values are provided in the figures or figure legends. Pearson correlation analysis was conducted to assess the association between NDUFA4 and miR-147b-3p.  $P < 0.05$  was considered statistically significant.

## Results

#### GEO dataset analysis and expression of miR-147b-3p

The GSE93883 and GSE74209 datasets were used for the analysis of differentially expressed microRNAs based on microRNA arrays. A log<sub>2</sub> fold change of  $>1$  and a Padj value of  $<0.05$  were set as the cutoff criteria. In the GSE93883 dataset, a total of 158 microRNAs were differentially expressed (Fig. 1A and C), while 138 microRNAs were differentially expressed in the GSE74209 dataset (Fig. 1B and D). The intersection of the differentially expressed miRNAs from both datasets identified 16

differentially expressed miRNAs (Fig. 1E). Among the 16 miRNAs, 6 miRNAs exhibited both up-regulation and down-regulation in the GSE93883 and GSE94702 datasets, including miR-147b-3p (Fig. 1F). Of these six miRNAs, miR-147b-3p was specifically chosen for further investigation due to its significantly lower expression in patients with osteoporotic vertebral compression fractures (OVCF) compared to controls (Fig. 1G, S1).

#### Effects of miR-147b-3p overexpression and inhibition on MC3T3-E1 cell osteogenic differentiation

To investigate the role of miR-147b-3p in osteogenic differentiation, MC3T3-E1 cells were transfected with either a miR-147b-3p mimic or a miR-147b-3p inhibitor to achieve overexpression or inhibition, respectively. qRT-PCR analysis confirmed the expression levels of miR-147b-3p following transfection (Fig. 2A). In MC3T3-E1 cells, miR-147b-3p overexpression significantly enhanced cell viability, whereas miR-147b-3p inhibition exerted the opposite effect (Fig. 2B). Subsequently, MC3T3-E1 cells were transfected with either the miR-147b-3p mimic or miR-147b-3p inhibitor and induced towards osteogenic differentiation for 14 days to evaluate the effects of miR-147b-3p on osteogenesis. On day 14 of osteogenic induction, Alizarin red staining revealed that miR-147b-3p overexpression significantly promoted osteoblast differentiation, whereas miR-147b-3p inhibition impaired the formation of mineralized nodules (Fig. 2C and D). Furthermore, ALP and RUNX2, two key mediators of osteogenic differentiation, were markedly upregulated in the miR-147b-3p mimic group, whereas the miR-147b-3p inhibitor group exhibited the opposite effect (Fig. 2E and F). These findings suggest that miR-147b-3p plays a crucial role in osteogenic differentiation by enhancing cell viability, promoting mineralized nodule formation, and upregulating osteogenic markers.

#### Inhibition of miR-147b-3p aggravated senile osteoporosis in mice

The senile osteoporosis murine model is commonly employed to examine age-related impairments in osteogenic function [18]. In this study, we developed the model using 6- and 18-month-old mice, which demonstrated tibial trabecular bone loss primarily evaluated via microcomputed tomography ( $\mu$ CT). To further validate our in vivo findings, the mice were subjected to a four-week treatment with either antagomir-miR-147b-3p or antagomir-control. Compared to the 6-month cohort, the 18-month cohort exhibited significant age-related trabecular bone loss and deterioration of bone microarchitecture. Suppression of miR-147b-3p resulted in additional reductions in trabecular bone mass and worsened microstructural integrity, characterized by decreased trabecular thickness, number, bone volume fraction, and

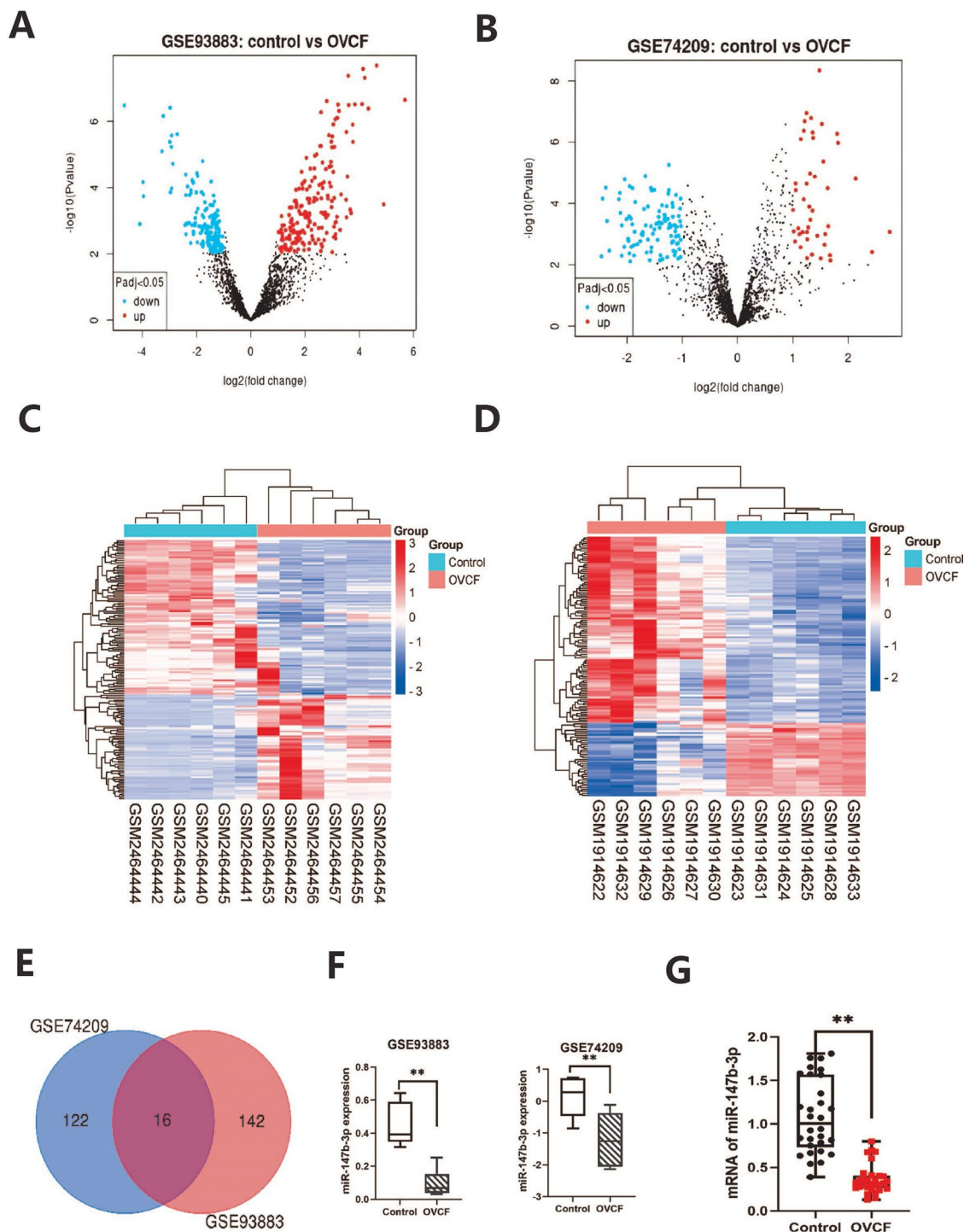


**Fig. 1** Differentially expressed microRNAs in GSE93883 and GSE74209. **(A,B)** volcano Plots of microRNAs by setting the cutoff as a log<sub>2</sub> fold change of > 1 and a P value of <0.05. Black color indicates non-significant microRNAs, while red or blue color represents up-regulated or down-regulated microRNAs. Heatmap of microRNA expression among six healthy(Control) and six OVCF samples in GSE93883 **(C)** and GSE74209 **(D)**. (Venn diagram of intersections of the differential miRNAs from GSE93883 and GSE74209. **(F)** mRNA level Of miR-147b-3p in healthy controls and OVCF in GSE93883 and GSE74209. **(G)** mRNA level Of miR-147b-3p in healthy controls and patients of OVCF

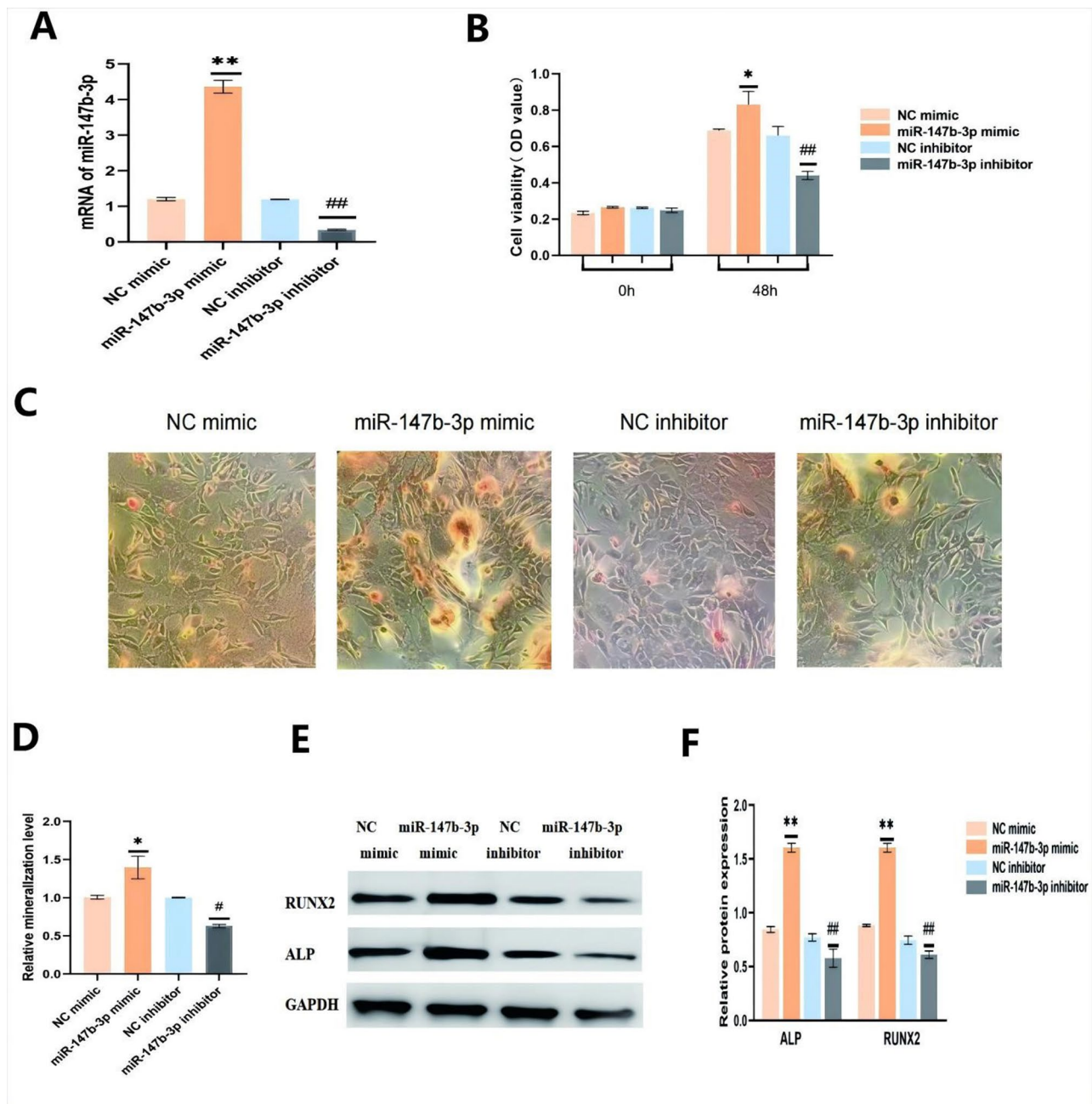


**Fig. 2** Effects of miR-147b-3p overexpression and inhibition on MC3T3-E1 cell osteogenic differentiation. **(A)** miR-147b-3p expression was confirmed using qRT-PCR. **(B)** MC3T3-E1 cells were transfected with miR-147b-3p mimic (50nM) or miR-147b-3p inhibitor (100nM) and examined for cell viability by CCK-8 assay. **(C, D)** Representative images of ARS staining of MC3T3-E1 cells treated with miR-147b-3p mimic or miR-147b-3p inhibitor in osteogenic induction medium for 14 days, respectively. Examined for the protein levels of ALP and Runx2 using immunoblotting on day 14 of osteogenic induction **(E, F)**. \* $P < 0.05$ , \*\* $P < 0.01$  compared to mimic NC, ## $P < 0.01$  compared to inhibitor NC

surface density, as well as increased trabecular separation and pattern factor (Fig. 3A and G). These results indicate that inhibition of miR-147b-3p exacerbates senile osteoporosis in mice.

#### MiR-147b-3p targeted on NDUFA4

Online databases (TargetScan and miRDB) were utilized to identify potential target genes of miR-147b-3p;

we identified a binding site between miR-147b-3p and the 3'-UTR of NDUFA4 mRNA (Fig. 4A). Dual luciferase reporter assays were performed to validate this interaction, demonstrating that transfection with the miR-147b-3p mimic resulted in a significant decrease in relative luciferase activity (RLA) for the wild-type NDUFA4 reporter plasmid but not for the mutant version (Fig. 4B). Furthermore, the miR-147b-3p inhibitor

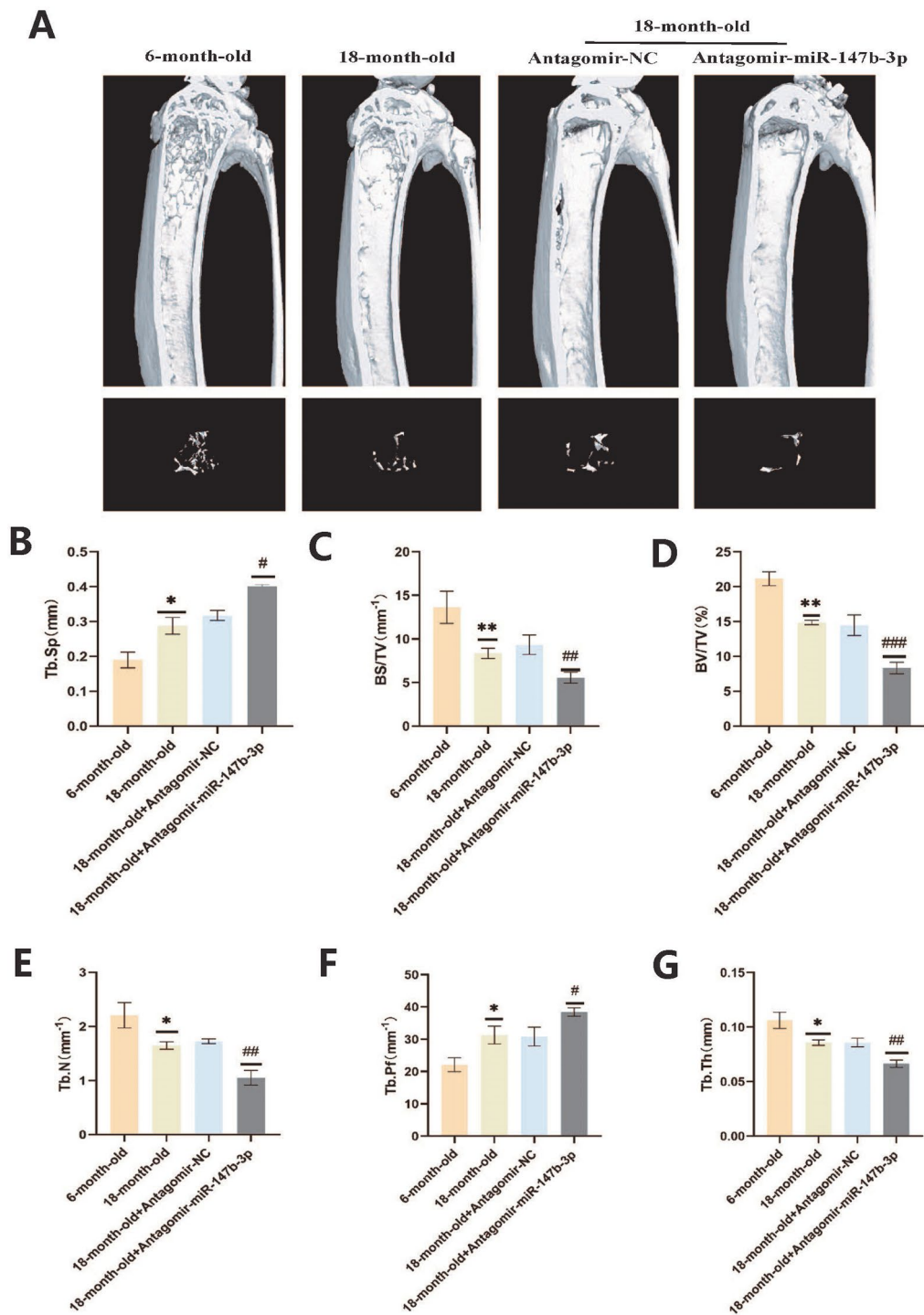


**Fig. 3** Inhibition of miR-147b-3p aggravated senile osteoporosis in mice. **(A)** Representative 3D reconstruction images of microarchitecture in the mice tibia. Groups are divided as follows: 6-month-old mice, 18-month-old mice, 18-month-old mice treated with antagomir-negative control (NC) and 18-month-old mice treated with antagomir-miR-147b-3p. **(B–G)** Micro-CT analysis includes trabecular separation (Tb.Sp), bone surface density (BS/TV), bone volume fraction (BV/TV), trabecular number (Tb.N), trabecular pattern factor (Tb.Pf), and trabecular thickness (Tb.Th). All data represent mean ± s.e.m. (n = 5). \*P < 0.05, \*\*P < 0.01 compared to the 6-month-old mice group. #P < 0.05, ###P < 0.01 compared to the group of 18-month-old mice treated with antagomir-NC

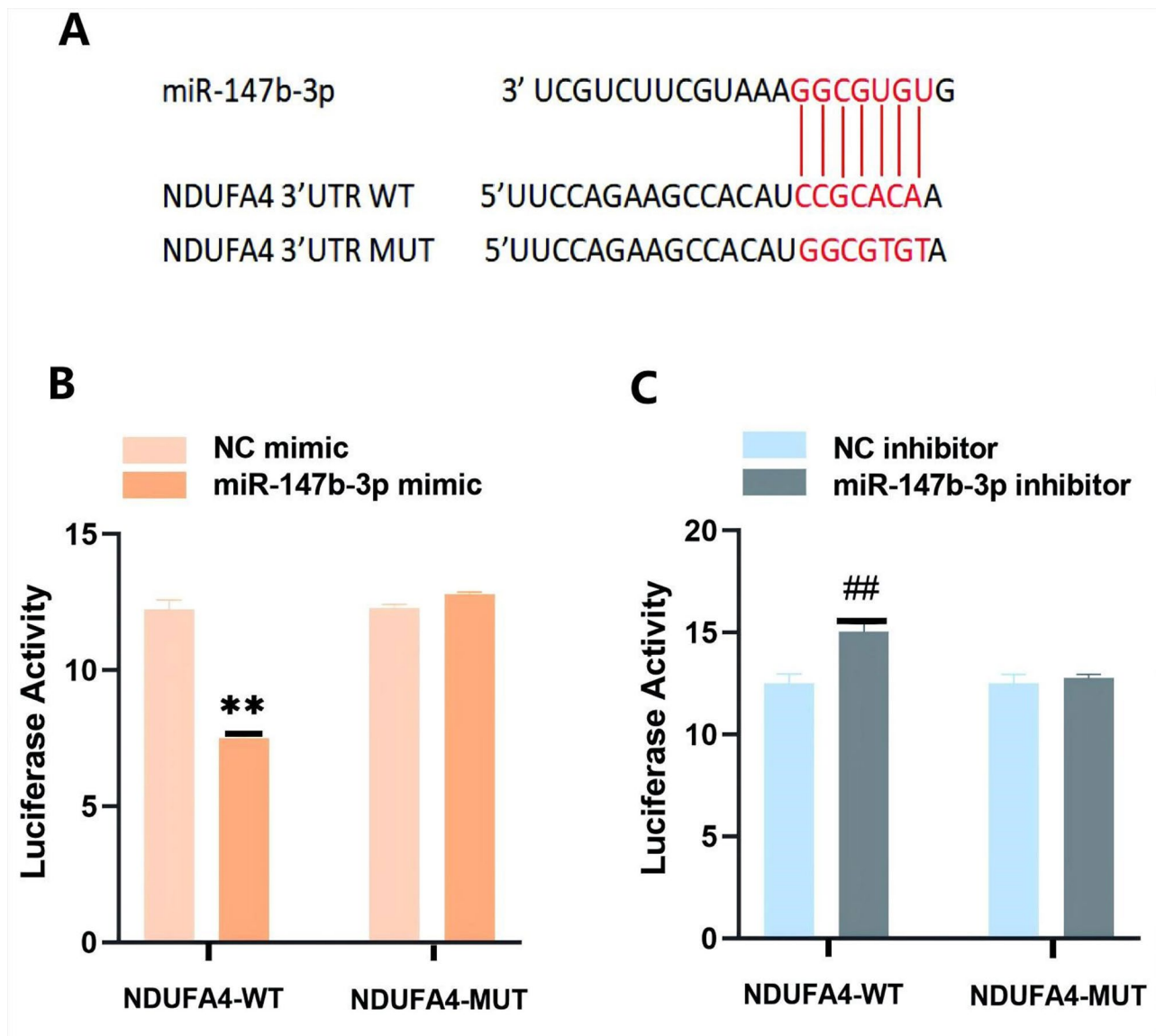


**Fig. 4** miR-147b-3p targeted NDUFA4. **(A)** The predicted sites of miR-147b-3p binding to the 3'-UTR of NDUFA4. **(B)** Luciferase activity was measured in miR-147b-3p mimic transfected 293T cells. **(C)** Luciferase activity was measured in miR-147b-3p inhibitor transfected 293T cells. Data were presented as mean  $\pm$  SD. \*\* $P < 0.01$  compared to NC mimic, ## $P < 0.01$  compared to NC inhibitor

enhanced RLA for a reporter plasmid containing only the WT 3'-UTR sequence rather than the MUT 3'-UTR of NDUFA4 (Fig. 4C). These results confirm that NDUFA4 is a direct target gene of miR-147b-3p.

#### Expression of miR-147b-3p and NDUFA4 in clinical specimens

The effects of miR-147b-3p and NDUFA4 on osteogenesis were investigated by comparing their expression levels in patients with and without osteoporotic vertebral compression fractures (OVCF). qRT-PCR results revealed that the miR-147b-3p expression level was lower (Fig. 5A) and that of NDUFA4 was greater (Fig. 5B) in patients with OVCF compared to the control. Besides,

Pearson correlation test unveiled a significant negative association between miR-147b-3p and NDUFA4 in both OVCF (Fig. 5C) and control patients (Fig. 5D), suggesting the participation of miR-147b-3p and NDUFA4 for the osteogenesis occurrence.

#### miR-147b-3p/NDUFA4 axis regulates the osteogenic differentiation in MC3T3-E1 cells

To investigate the biological function of miR-147b-3p and NDUFA4 in osteogenic differentiation, an NDUFA4 overexpression plasmid (p-NDUFA4) was transfected into MC3T3-E1 cells, leading to a significant upregulation of NDUFA4 expression. This was confirmed by qRT-PCR analysis, which demonstrated increased NDUFA4

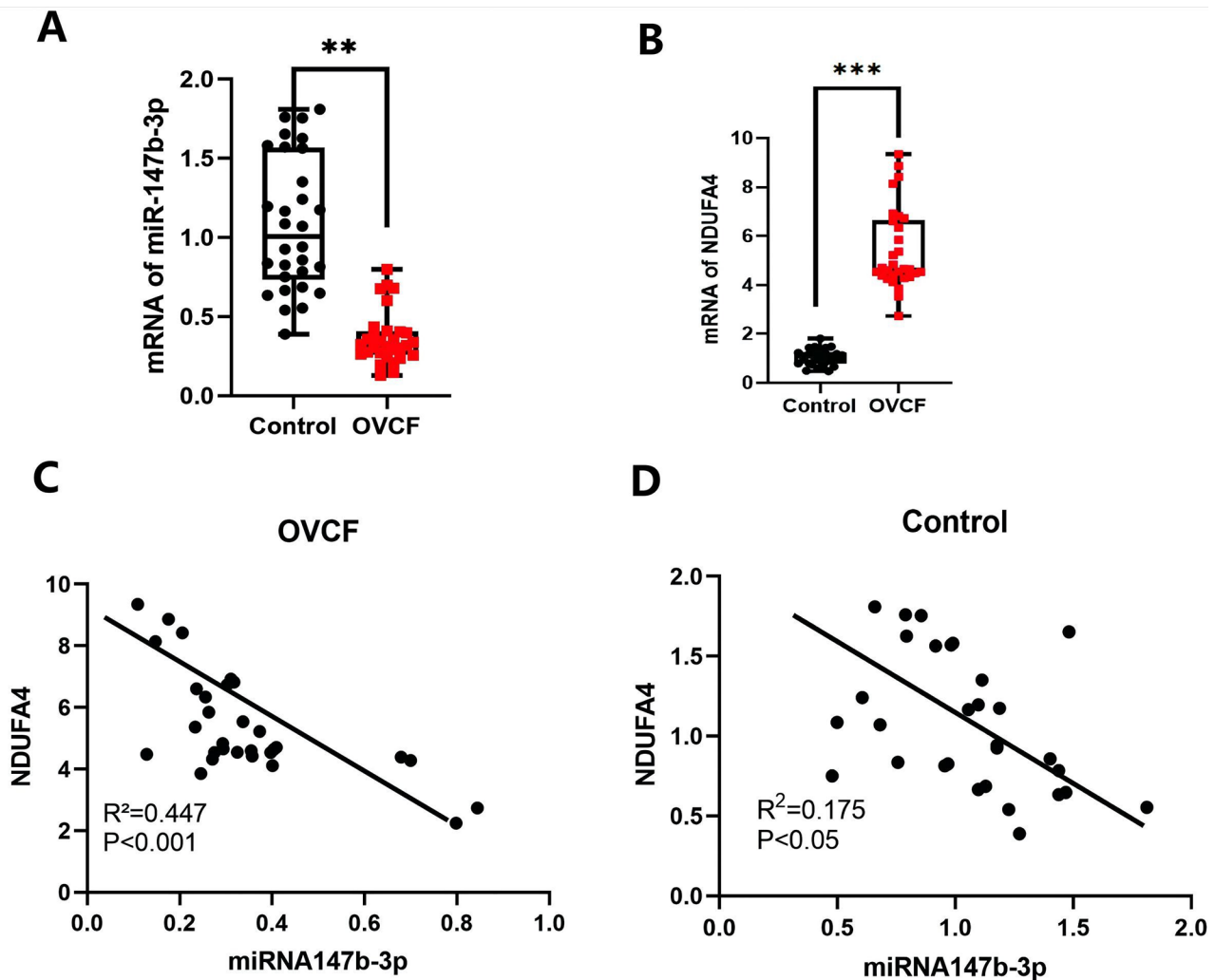


**Fig. 5** Expressions of miR-147b-3p and NDUFA4 in clinical samples. (A) Expressions of miR-147b-3p in patients with or without OVCF. (B) Expressions of NDUFA4 in patients with or without OVCF. (C) Pearson correlation analysis of miR-147b-3p expression and NDUFA4 in OVCF samples. (D) Pearson correlation analysis of miR-147b-3p expression and NDUFA4 in control samples. Data were presented as mean  $\pm$  SD

gene expression (Fig. 6A). Subsequently, MC3T3-E1 cells were co-transfected with p-NDUFA4 and miR-147b-3p mimic to assess their impact on NDUFA4 protein levels. Western blot analysis revealed that the miR-147b-3p mimic reduced NDUFA4 protein expression, whereas NDUFA4 overexpression led to its increase. Notably, the inhibitory effect of miR-147b-3p on NDUFA4 protein expression was counteracted by NDUFA4 overexpression (Fig. 6B and C). Additionally, miR-147b-3p mimic significantly enhanced cell viability, whereas NDUFA4 overexpression suppressed cell viability. More importantly, NDUFA4 overexpression effectively mitigated the pro-cell viability effect exerted by miR-147b-3p (Fig. 6D). For further validation, a co-transfection approach involving both p-NDUFA4 and miR-147b-3p mimic was employed in MC3T3-E1 cells, followed by osteogenic differentiation induction for 14 days. Alizarin red staining demonstrated that the miR-147b-3p mimic significantly enhanced

osteoblast differentiation on day 14 of induction, whereas NDUFA4 overexpression impaired mineralized nodule formation. Notably, the osteogenic-promoting effect of miR-147b-3p was attenuated by NDUFA4 overexpression (Fig. 6E and F). Similarly, on day 14 of osteogenic induction, the miR-147b-3p mimic markedly upregulated the expression of ALP and Runx2, whereas NDUFA4 overexpression led to a reduction in ALP and Runx2 levels. Again, the osteogenic-promoting effect of miR-147b-3p on ALP and Runx2 expression was significantly weakened by NDUFA4 overexpression (Fig. 6G and H). Collectively, these findings suggest that miR-147b-3p modulates bone formation in MC3T3-E1 cells by targeting NDUFA4.

#### PI3K-Akt pathway is found in gene ontology (GO) and KEGG pathway enrichment analysis

The target genes of differentially expressed miRNAs in the GSE93883 and GSE74209 datasets were predicted

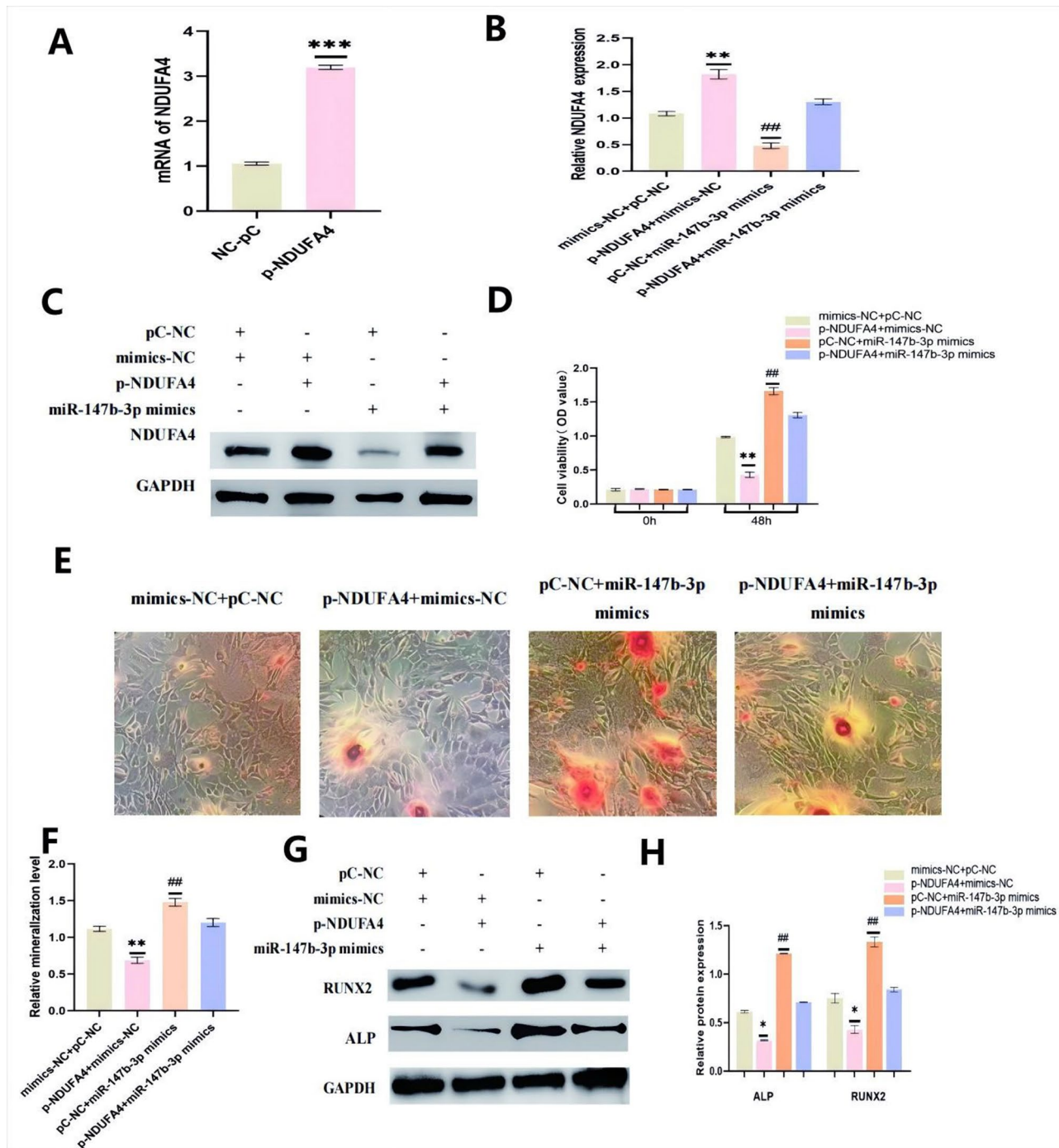


**Fig. 6** The miR-147b-3p/NDUFA4 axis regulates the osteogenic differentiation in MC3T3-E1 cells. **(A)**The transfection efficiency of p-NDUFA4 was detected by qRT-PCR. Subsequently, co-transfection of NDUFA4 overexpression (p-NDUFA4) and miR-147b-3p mimic was performed in MC3T3-E1 cells. Western blotting analysis **(B,C)** revealed expression levels of NDUFA4 protein, while cell viability was assessed using the CCK-8**(D)**.Then, MC3T3-E1 cells were co-transfected with p-NDUFA4 and miR-147b-3p mimic and induced for osteogenic differentiation for 14 days. Alizarin red staining **(E,F)** allowed observation of mineralized nodule formation during osteogenesis induction.Western blotting analysis of osteogenic induction demonstrated levels of ALP and Runx2 proteins **(G,H)**. Data were presented as mean  $\pm$  SD. \* $P < 0.05$ , \*\* $P < 0.01$ , \*\*\* $P < 0.001$  compared to NC, ## $P < 0.01$  compared to NC

using the MiRDB, TargetScan, and miRWALK databases. Subsequently, a total of 596 gene symbols were identified for subsequent KEGG and GO analysis. The GO functional analysis encompassed cell components

(CC), biological processes (BP), and molecular functions (MF) (Fig. 7A and C). MF analysis showed (Fig. 7C) high enrichment of DNA-binding transcription factor binding, nuclear receptor activity, and transcription

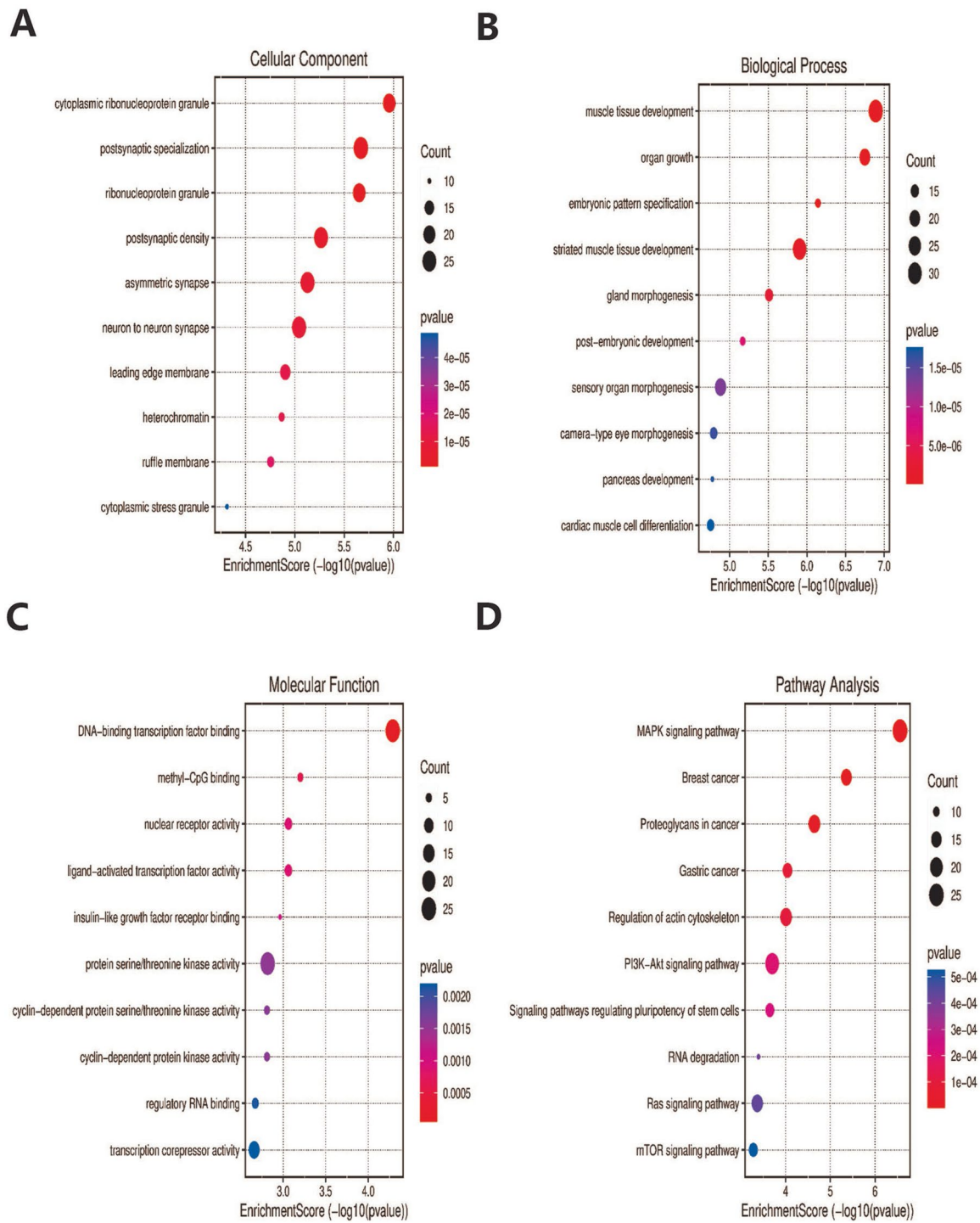


**Fig. 7** GO and KEGG pathway enrichment analysis. **(A-C)** GO enrichment analysis was carried out using CC, BP, and MF. **(D)** KEGG pathway analysis of the DEGs. The x-axis shows enriched gene numbers, and the color represents significance. GO terms are shown on the y-axis

corepressor activity, consistent with the recognition of a wide range of microRNA functions. BP analysis showed (Fig. 7B) that pathways such as muscle tissue development and organ growth were highly enriched, indicating that these microRNAs were potentially involved in bone formation. The KEGG pathway enrichment analysis revealed significant enrichment of these microRNAs in key signaling pathways, including MAPK, PI3K-Akt, Ras, mTOR, and others (Fig. 7D).

#### The PI3K/AKT pathway is involved in the osteogenic differentiation mediated by the miR-147b-3p/NDUFA4 axis

To examine the molecular mechanisms of miR-147b-3p and NDUFA4 in osteogenic differentiation, combined with the results of KEGG pathway enrichment analysis, the downstream cascade PI3K/AKT pathway was analyzed. The miR-147b-3p mimic markedly enhanced the PI3K (p-PI3K) and AKT (p-AKT) phosphorylation levels in comparison with the control group (Fig. 8A and C), thereby miR-147b-3p mimics activated this pathway. Conversely, overexpression of NDUFA4 reduced the PI3K phosphorylation (p-PI3K) and AKT phosphorylation (p-AKT) levels (Fig. 8A and C) and suppressed the PI3K/AKT signaling pathway. However, miR-147b-3p mimics and NDUFA4 overexpression reversed the upregulation of both p-AKT and p-PI3K, which had been induced by miR-147b-3p mimics. These findings indicate that the PI3K/AKT pathway is implicated in osteogenic differentiation and is regulated by the miR-147b-3p/NDUFA4 axis in MC3T3-E1 cells.

In summary, our study demonstrated that miR-147b-3p overexpression promotes osteoblast differentiation by enhancing the expression of ALP and RUNX2, two key mediators of osteogenic differentiation. Furthermore, miR-147b-3p regulates bone formation in MC3T3-E1 cells by targeting NDUFA4. Notably, transfection with miR-147b-3p mimics significantly increased PI3K phosphorylation (p-PI3K) and AKT phosphorylation (p-AKT) levels, whereas NDUFA4 overexpression led to their reduction. These findings suggest that miR-147b-3p influences the progression of osteoporosis by targeting NDUFA4 and modulating the PI3K/AKT signaling pathway (Fig. 9).

#### Discussion

In this study, we identified miR-147b-3p as a differentially expressed miRNA in OVCF patients based on analyses of two GEO datasets and subsequently investigated its functional role both *in vitro* and *in vivo*. The dual luciferase reporter gene assay confirmed that NDUFA4 is a direct target of miR-147b-3p. Our experimental results demonstrated that miR-147b-3p mimics promoted osteogenic differentiation, whereas miR-147b-3p inhibitors and NDUFA4 overexpression exhibited inhibitory

effects. Furthermore, inhibition of miR-147b-3p using antagomir-miR-147b-3p exacerbated senile osteoporosis in mice, underscoring its potential regulatory role in bone homeostasis. Additionally, our findings revealed that the miR-147b-3p/NDUFA4 axis modulates the PI3K/AKT signaling pathway in MC3T3-E1 cells, suggesting its involvement in the molecular mechanisms underlying osteogenic differentiation and osteoporosis progression.

Previous studies have demonstrated a correlation between miRNA dysregulation and various diseases, including osteoporosis [19–22]. An increasing number of miRNAs have been identified as potential therapeutic targets or diagnostic biomarkers for osteoporosis [23–25]. In this study, we focused on osteoporotic vertebral fractures, a severe complication of osteoporosis, to investigate the impact of different miRNAs on osteogenic differentiation. Through bioinformatics analysis, miR-147b-3p was identified from the GEO dataset, as it was significantly downregulated in patients with osteoporotic vertebral fractures. By manipulating the expression of miR-147b-3p in MC3T3-E1 cells, we discovered its regulatory effect on osteogenic differentiation.

Additionally, a recent study investigated the role of microRNA-147 in rheumatoid arthritis and experimental arthritis, demonstrating that the loss of microRNA-147 function alleviates synovial inflammation by targeting ZNF148. Furthermore, anti-miR-147 therapy has been shown to reduce the severity of arthritis, particularly in experimental arthritis characterized by synovitis and joint destruction [26]. Another study identified potential mRNA and non-coding RNA targets using full transcriptome sequencing, combined with miRanda and RNAhybrid prediction algorithms. This analysis predicted a specific RNA regulatory axis involving hsa\_circ\_0018069-miR-147b-3p-TJP2, suggesting its potential as a novel target for early treatment of degenerative meniscus disease [27].

NADH: ubiquinone oxidoreductase subunit A4 (NDUFA4) is an essential protein involved in electron transfer within the mitochondrial respiratory chain of mammalian cells. As a crucial subunit of cytochrome C oxidase (COX), NDUFA4 participates in energy transfer at the terminal stage of the respiratory chain, playing a vital role in cellular energy metabolism [28]. Studies have demonstrated increased expression of NDUFA4 in various cancers, including colorectal cancer and lung cancer, where it contributes to tumor progression by influencing oxidative phosphorylation within tumor cells [29, 30]. For example, NDUFA4 is upregulated in head and neck paraganglioma, and its knockdown disrupts mitochondrial respiratory chain assembly, reduces ATP production, and attenuates cancer cell viability, suggesting that NDUFA4 promotes tumor progression in head and neck paraganglioma [31]. Zhu et al. demonstrated that miR-147 was

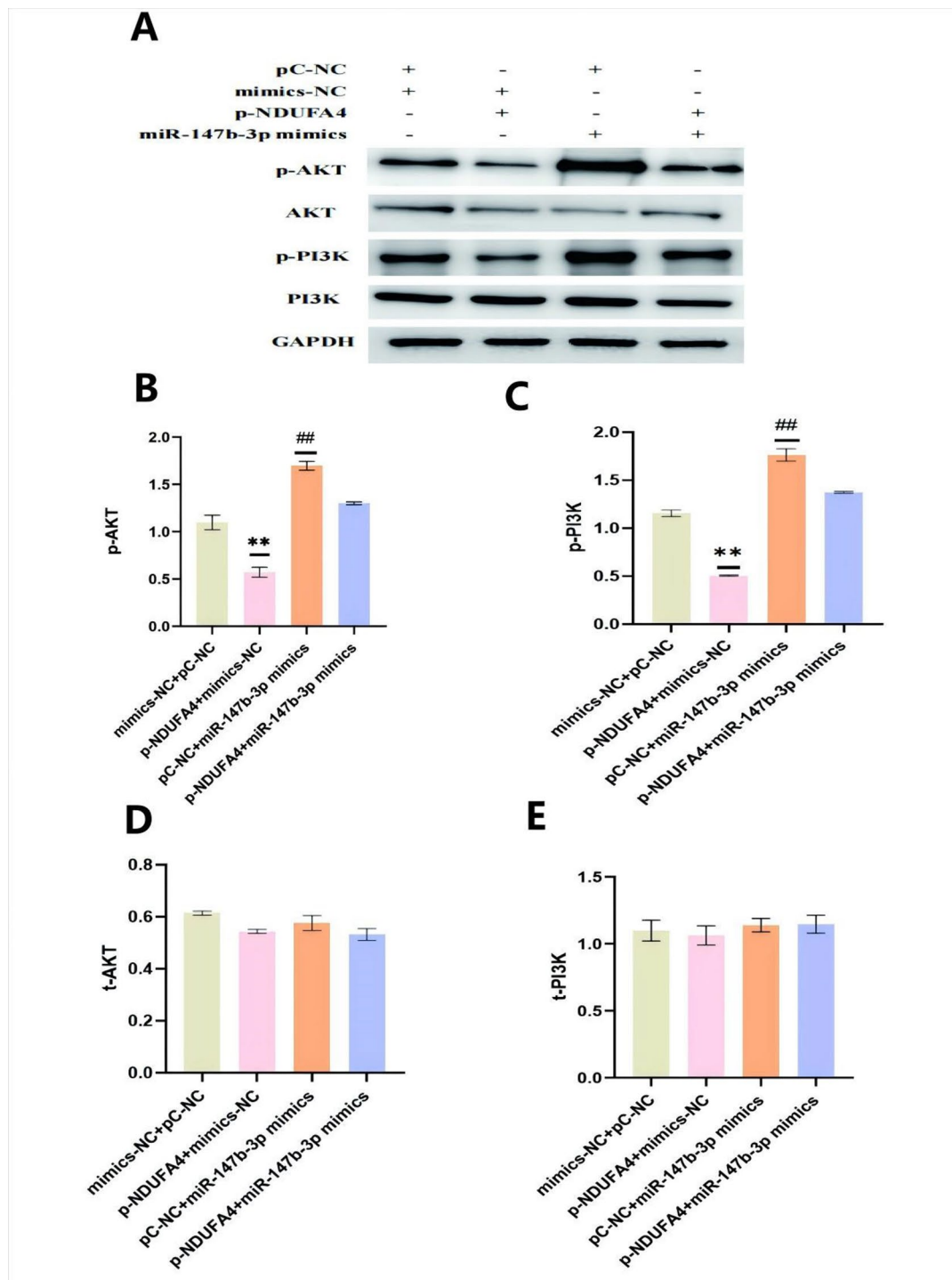


**Fig. 8** The PI3K/AKT pathway is involved in the osteoporosis mediated by the miR-147b-3p/NDUFA4 axis. **(A)** Western blotting results of p-PI3K, PI3K, p-AKT, and AKT in MC3T3-E1 cells. **(B-E)** Quantitative analysis of the optical density in **(A)**. Data were presented as mean ± SD. \*\**P* < 0.01 compared to NC, ##*P* < 0.01 compared to NC

persistently upregulated during cold storage-associated transplantation (CST) injury in both mouse models and human kidney transplants with dysfunction. Their study further identified NDUFA4 as a direct target gene of miR-147. Inhibition of miR-147 and upregulation of

NDUFA4 were shown to mitigate CST-induced damage and improve graft function. Conversely, NDUFA4 suppression exacerbated tubular cell death, whereas NDUFA4 overexpression prevented miR-147-induced cell death and mitochondrial dysfunction [32]. However,

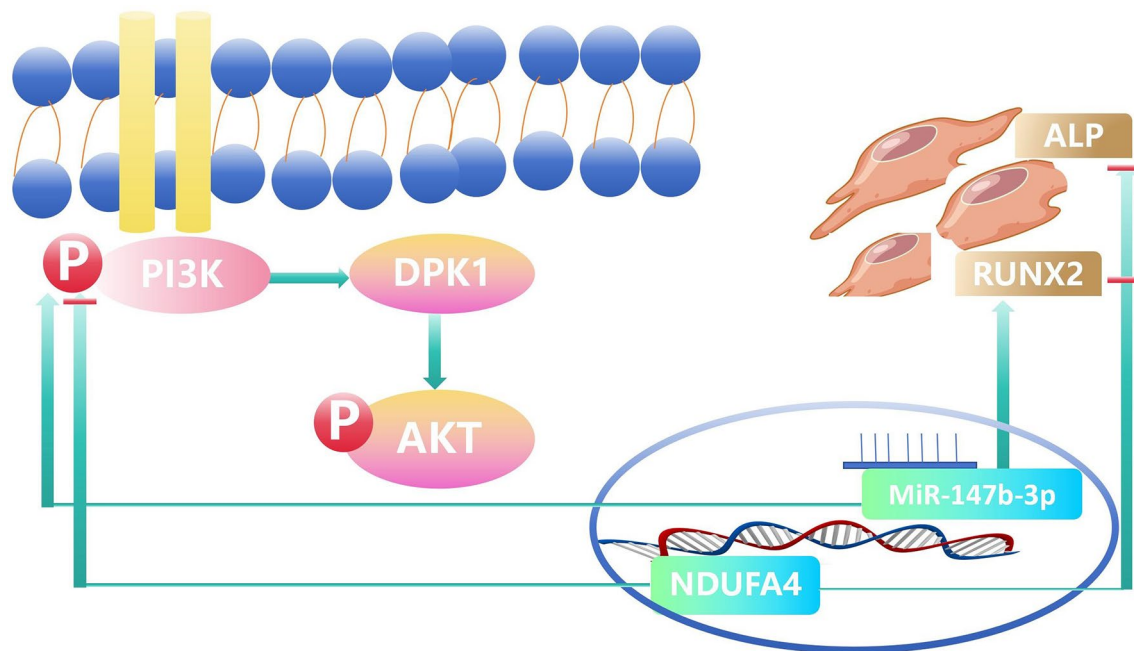


**Fig. 9** miR-147b-3p exerts an influence on the progression of osteoporosis by targeting NDUFA4 and regulating the PI3K/AKT signaling pathway

the relationship between miR-147b-3p and/or NDUFA4 with osteoporosis or osteoporotic vertebral fractures has not been previously reported.

This study confirmed that NDUFA4 is the direct target gene of miR-147b-3p through luciferase reporter gene assays. The overexpression of NDUFA4 in MC3T3-E1 cells was verified, and its impact on the osteogenic differentiation of MC3T3-E1 cells was investigated. Our findings indicate that miR-147b-3p affects osteoblast function in MC3T3-E1 cells by targeting NDUFA4. To further explore the mechanism of the miR-147b-3p/NDUFA4 axis in osteoporotic vertebral fractures, we examined relevant signaling pathways. The PI3K/AKT signaling pathway has been extensively studied for its crucial role in regulating osteoblast proliferation, differentiation, and apoptosis [33–37]. Dong et al. reported that ICG001, a  $\beta$ -catenin transcriptional activity inhibitor, suppresses the proliferation, differentiation, and mineralization of osteoblasts induced by PI3K/AKT activation. Furthermore, they demonstrated that the PI3K/AKT pathway plays a pivotal role in fracture healing and promotes fracture repair [38]. Recent studies have shown that the upregulation of miR-4739 is implicated in osteoporosis progression by targeting ITGA10 and regulating the PI3K/AKT signaling pathway. The miR-4739/ITGA10 axis has been suggested as a potential diagnostic marker and therapeutic target for osteoporosis [39]. Additionally, silencing miR-483-5p alleviates postmenopausal osteoporosis by targeting SATB2 and the PI3K/AKT pathway [15]. miR-140-3p targets PTEN, leading to its downregulation. Inhibition of miR-140-3p promotes

proliferation, differentiation, and apoptosis resistance in CD14+ PBMCs. Conversely, inhibition of PTEN via miR-140-3p activates the PTEN/PI3K/AKT signaling pathway, thereby promoting proliferation and differentiation while inhibiting apoptosis in C2C12 cells [40]. Consistent with these findings, KEGG pathway enrichment analysis revealed that multiple microRNAs are significantly enriched in key signaling pathways, including PI3K/AKT. Therefore, we hypothesize that the effect of the miR-147b-3p/NDUFA4 axis on osteoporotic vertebral fractures may be associated with the modulation of the PI3K/AKT signaling pathway. To test this hypothesis, we manipulated the expression levels of miR-147b-3p in vitro and assessed alterations in PI3K and AKT phosphorylation, as well as their effects on osteogenic markers. Our experimental results demonstrated that miR-147b-3p mimics activate the PI3K/AKT signaling pathway and enhance the expression of RUNX2 and ALP, suggesting that downregulation of miR-147b-3p impairs osteoblast activity and differentiation via NDUFA4 and the PI3K/AKT signaling pathway.

Although our study provides experimental evidence using MC3T3-E1 cells and a limited set of in vivo experiments, these models may not fully replicate the characteristics of osteoblasts in osteoporosis and vertebral fractures. Therefore, further validation with larger sample sizes, particularly in in vivo studies, as well as multicenter clinical research, is essential to comprehensively substantiate our findings. In conclusion, our study demonstrated that miR-147b-3p is downregulated in osteoporotic vertebral fractures and influences the progression

of osteoporosis and vertebral fractures by targeting NDUFA4 and regulating the PI3K/AKT signaling pathway. These findings provide novel insights into the molecular mechanisms underlying osteoporotic vertebral fractures, offering theoretical support for the potential use of the miR-147b-3p/NDUFA4 axis as a target for both diagnosis and treatment.

### Supplementary Information

The online version contains supplementary material available at <https://doi.org/10.1186/s13018-025-05598-2>.

Supplementary Material 1

### Acknowledgements

Not applicable.

### Author contributions

SK, LZJ, and GYY performed the experiments and analyzed the data. GYY wrote the article. LZJ and GYY performed the bioinformatics analysis and revised the article. NCC and LY designed the study and reviewed the article. All authors read and approved the final manuscript as submitted.

### Funding

This work was supported by grants for the Science and Technology and Health Commission program of Chongqing (2020FYYX157); Chongqing Health Commission and Science and Technology Bureau (2024MSXM105); Tibet Autonomous Region Science and Technology Plan Projects (XZ202301YD0001C).

### Data availability

No datasets were generated or analysed during the current study.

### Declarations

#### Ethics approval and consent to participate

All primary samples were obtained from the Spinal Surgery Department of Chongqing General Hospital under protocols approved by the Ethics Committee of Chongqing General Hospital (approval No. KY2021-033-01). Written informed consent was obtained from all patients.

#### Competing interests

The authors declare no competing interests.

#### Author details

<sup>1</sup>Chongqing Medical University, Chongqing 400016, China

<sup>2</sup>Department of Laboratory Medicine, Chongqing General Hospital, Chongqing University, Chongqing 401147, China

<sup>3</sup>Department of Spine Surgery, Chongqing General Hospital, Chongqing University, Chongqing 401147, China

<sup>4</sup>Chongqing Key Laboratory of Reproductive Health and Digital Medicine, Department of Laboratory Medicine, Chongqing General Hospital, School of Medicine, Chongqing University, Chongqing 401147, China

<sup>5</sup>College of Life Science and Laboratory Medicine, Kunming Medical University, Kunming, Yunnan 650050, China

Received: 12 January 2025 / Accepted: 10 February 2025

Published online: 04 March 2025

### References

- Zhang S, Lee Y, Liu Y, Yu Y, Han I. Stem cell and regenerative therapies for the treatment of Osteoporotic Vertebral Compression fractures. *Int J Mol Sci*. 2024;25(9):4979. <https://doi.org/10.3390/ijms25094979>. PMID: 38732198.
- Pfeifle C, Kohut P, Jarvers JS, Spiegel UJ, Heyde CE, Osterhoff G. Does time-to-surgery affect mortality in patients with acute osteoporotic vertebral compression fractures? *BMC Geriatr*. 2021;21(1):714. <https://doi.org/10.1186/s12877-021-02682-0>. PMID: 34922479.
- Nakahama K. Cellular communications in bone homeostasis and repair. *Cell Mol Life Sci*. 2010; 67(23): 4001-9. <https://doi.org/10.1007/s00018-010-0479-3>. PMID: 20694737.
- Du X, Zang C, Wang Q. Cyclin A1 (CCNA1) inhibits osteoporosis by suppressing transforming growth factor-beta (TGF-beta) pathway in osteoblasts. *BMC Musculoskelet Disord*. 2024;25(1):206. <https://doi.org/10.1186/s12891-024-07303-6>. PMID: 38454404.
- Bellavia D, De Luca A, Carina V, Costa V, Raimondi L, Salamanna F, Alessandro R, Fini M, Giavaresi G. Deregulated miRNAs in bone health: Epigenetic roles in osteoporosis. *Bone*. 2019;122:52-75. <https://doi.org/10.1016/j.bone.2019.02.013>. PMID: 30772601.
- Lu TX, Rothenberg ME. MicroRNA. *J Allergy Clin Immunol*. 2018;141(4):1202-1207. <https://doi.org/10.1016/j.jaci.2017.08.034>. PMID: 29074454.
- Mohr AM, Mott JL. Overview of microRNA biology. *Semin Liver Dis*. 2015;35(1):3-11. <https://doi.org/10.1055/s-0034-1397344>. PMID: 25632930.
- Kumar V, Gautam M, Chaudhary A, Chaurasia B. Impact of three miRNA signature as potential diagnostic marker for triple negative breast cancer patients. *Sci Rep*. 2023;13(1):21643. <https://doi.org/10.1038/s41598-023-48896-7>. PMID: 38062163.
- Zhang X, Xu J. A novel miR-4661-3p/FGF23 axis promotes osteogenic differentiation of human bone marrow mesenchymal stem cells. *Bone*. 2024;117:123. <https://doi.org/10.1016/j.bone.2024.117123>. PMID: 38735373.
- Giordano L, Porta GD, Peretti GM, Maffulli N. Therapeutic potential of microRNA in tendon injuries. *Br Med Bull*. 2020;133(1):79-94. <https://doi.org/10.1093/bmb/ldaa002>. PMID: 32219416.
- Oliviero A, Della Porta G, Peretti GM, Maffulli N. MicroRNA in osteoarthritis: physiopathology, diagnosis and therapeutic challenge. *Br Med Bull*. 2019;130(1):137-147. <https://doi.org/10.1093/bmb/ldz015>. Erratum in: *Br Med Bull*. 2022;144(1):90. <https://doi.org/10.1093/bmb/ldz021>. PMID: 31066454.
- Gargano G, Oliva F, Oliviero A, Maffulli N. Small interfering RNAs in the management of human rheumatoid arthritis. *Br Med Bull*. 2022;142(1):34-43. <https://doi.org/10.1093/bmb/ldac012>. PMID: 35488320; PMCID: PMC9351475.
- Long Z, Dou P, Cai W, Mao M, Wu R. MiR-181a-5p promotes osteogenesis by targeting BMP3. *Aging*. 2023;15(3):734-47. <https://doi.org/10.18632/aging.204505>. PMID: 36734882
- Li D, Yuan Q, Xiong L, Li A, Xia Y. The miR-4739/DLX3 Axis Modulates Bone Marrow-Derived Mesenchymal Stem Cell (BMSC) Osteogenesis Affecting Osteoporosis Progression. *Front Endocrinol (Lausanne)*. 2021;12:703167. <https://doi.org/10.3389/fendo.2021.703167>. PMID: 34925225.
- Zhao F, Xu Y, Ouyang Y, Wen Z, Zheng G, Wan T, Sun G. Silencing of mir-483-5p alleviates postmenopausal osteoporosis by targeting SATB2 and PI3K/AKT pathway. *Aging*. 2021;13(5):6945-56. <https://doi.org/10.18632/aging.202552>. PMID: 33621956.
- Wang X, Guo B, Li Q, Peng J, Yang Z, Wang A, Li D, Hou Z, Lv K, Kan G, Cao H, Wu H, Song J, et al. miR-214 targets ATF4 to inhibit bone formation. *Nat Med*. 2013;19(1):93-100. <https://doi.org/10.1038/nm.3026>. Epub 2012 Dec 9. PMID: 23223004.
- Banovac I, Grgurevic L, Rumenovic V, Vukicevic S, Erjavec I. BMP3 affects cortical and trabecular long bone development in mice. *Int J Mol Sci*. 2022; 23(2):785. <https://doi.org/10.3390/ijms23020785>. PMID: 35054971.
- Jilka RL. The relevance of mouse models for investigating age-related bone loss in humans. *J Gerontol Biol Sci Med Sci*. 2013;68:1209-17. <https://doi.org/10.1093/gerona/glt046>. PMID:23689830.
- Gargano G, Oliviero A, Oliva F, Maffulli N. Small interfering RNAs in tendon homeostasis. *Br Med Bull*. 2021;138(1):58-67. <https://doi.org/10.1093/bmb/ldaa040>. PMID: 33454750.
- Wang H, Shi MJ, Hu ZQ, Miao L, Cai HS, Zhang RP. Effect of miR-206 on lower limb ischemia-reperfusion injury in rat and its mechanism. *Sci Rep*. 2023;13(1):21574. <https://doi.org/10.1038/s41598-023-48858-z>. PMID: 38062081.
- Li D, Luo C, Deng J, Xu Y, Fu S, Liu K, Wu J. MicroRNA 211-5p inhibits cancer cell proliferation and migration in pancreatic cancer by targeting BMP2. *Aging (Albany, NY)*. 2023;15(23):14411-14421. <https://doi.org/10.18632/aging.205320>. PMID: 38059889.
- Wang G, Wan L, Zhang L, Yan C, Zhang Y. MicroRNA-133a Regulates the Viability and Differentiation Fate of Bone Marrow Mesenchymal Stem

- Cells via MAPK/ERK Signaling Pathway by Targeting FGFR1. *DNA Cell Biol.* 2021;40(8):1112–1123. <https://doi.org/10.1089/dna.2021.0206>. PMID: 34165368.
23. Gargano G, Asparago G, Spiezia F, Oliva F, Maffulli N. Small interfering RNAs in the management of human osteoporosis. *Br Med Bull.* 2023;148(1):58–69. <https://doi.org/10.1093/bmb/ldad023>. PMID: 37675799; PMCID: PMC10788844.
  24. Taipaleenmäki H, Saito H, Schröder S, Maeda M, Mettler R, Ring M, Rollmann E, Gasser A, Haasper C, Gehrke T, Weiss A, Grimm SK, Hesse E. Antagonizing microRNA-19a/b augments PTH anabolic action and restores bone mass in osteoporosis in mice. *EMBO Mol Med.* 2022;14(11):e13617. <https://doi.org/10.15252/emmm.202013617>. PMID: 36193848.
  25. Zhao X, Zhao D, Geng B, Yaobin W, Xia Y. A novel ceRNA regulatory network involving the long noncoding NEAT1, miRNA-466f-3p and its mRNA target in osteoblast autophagy and osteoporosis. *J Mol Med (Berl).* 2022;100(11):1629–1646. <https://doi.org/10.1007/s00109-022-02255-7>. PMID: 36169673.
  26. Jiang C, Wu X, Li X, Li M, Zhang W, Tao P, Xu J, Ren X, Mo L, Guo Y, Wang S, Geng M, Zhang F, Tian J, Zhu W, Meng L, Lu S. Loss of microRNA-147 function alleviates synovial inflammation through ZNF148 in rheumatoid and experimental arthritis. *Eur J Immunol.* 2021;51(8):2062–2073. <https://doi.org/10.1002/eji.202048850>. PMID: 33864383.
  27. Jiang Z, Du X, Wen X, Li H, Zeng A, Sun H, Hu S, He Q, Liao W, Zhang Z. Whole-Transcriptome Sequence of Degenerative Meniscus Cells Unveiling Diagnostic Markers and Therapeutic Targets for Osteoarthritis. *Front Genet.* 2021;12:754421. <https://doi.org/10.3389/fgene.2021.754421>. PMID: 34721542.
  28. Zhou Q, Li X, Zhou H, Zhao J, Zhao H, Li L, Zhou Y. Mitochondrial respiratory chain component NDUFA4: a promising therapeutic target for gastrointestinal cancer. *Cancer Cell Int.* 2024;24(1):97. <https://doi.org/10.1186/s12935-024-03283-8>. PMID: 38443961.
  29. Cui S, Yang X, Zhang L, Zhao Y, Yan W. LncRNA MAFG-AS1 promotes the progression of colorectal cancer by sponging miR-147b and activation of NDUFA4. *Biochem Biophys Res Commun.* 2018;506(1):251–258. <https://doi.org/10.1016/j.bbrc.2018.10.112>. PMID: 30348529.
  30. Lei L, Chen C, Zhao J, Wang H, Guo M, Zhou Y, Luo J, Zhang J, Xu L. Targeted Expression of miR-7 Operated by TTF-1 Promoter Inhibited the Growth of Human Lung Cancer through the NDUFA4 Pathway. *Mol Ther Nucleic Acids.* 2017;6:183–197. <https://doi.org/10.1016/j.omtn.2016.12.005>. PMID: 28325285.
  31. Wang Z, Tao E, Chen Y, Wang Q, Liu M, Wei L, Xu S, Chen W, Zhong C. NDUFA4 promotes the progression of head and neck paraganglioma by inhibiting ferroptosis. *Biochem Cell Biol.* 2023;101(6):523–530. <https://doi.org/10.1139/bcb-2023-0018>. PMID: 37602474.
  32. Zhu J, Xiang X, Hu X, Li C, Song Z, Dong Z. miR-147 Represses NDUFA4, Inducing Mitochondrial Dysfunction and Tubular Damage in Cold Storage Kidney Transplantation. *J Am Soc Nephrol.* 2023;34(8):1381–1397. <https://doi.org/10.1681/ASN.000000000000154>. PMID: 37211637.
  33. Li Z, Li Y, Liu C, Gu Y, Han G. Research progress of the mechanisms and applications of ginsenosides in promoting bone formation. *Phytomedicine.* 2024;129:155604. <https://doi.org/10.1016/j.phymed.2024.155604>. PMID: 38614042.
  34. Chai S, Yang Y, Wei L, Cao Y, Ma J, Zheng X, Teng J, Qin N. Luteolin rescues postmenopausal osteoporosis elicited by OVX through alleviating osteoblast pyroptosis via activating PI3K-AKT signaling. *Phytomedicine.* 2024;128:155516. <https://doi.org/10.1016/j.phymed.2024.155516>. PMID: 38547625.
  35. Zheng HL, Xu WN, Zhou WS, Yang RZ, Chen PB, Liu T, Jiang LS, Jiang SD. Beraprost ameliorates postmenopausal osteoporosis by regulating Nedd4-induced Runx2 ubiquitination. *Cell Death Dis.* 2021;12(5):497. <https://doi.org/10.1038/s41419-021-03784-8>. PMID: 33993186.
  36. Xu J, Fu L, Bai J, Zhong H, Kuang Z, Zhou C, Hu B, Ni L, Ying L, Chen E, Zhang W, Wu J, Xue D, Li W, Pan Z. Low-dose IL-34 has no effect on osteoclastogenesis but promotes osteogenesis of hBMSCs partly via activation of the PI3K/AKT and ERK signaling pathways. *Stem Cell Res Ther.* 2021;12(1):268. <https://doi.org/10.1186/s13287-021-02263-3>. PMID: 33947456.
  37. Zhao B, Peng Q, Poon EHL, Chen F, Zhou R, Shang G, Wang D, Xu Y, Wang R, Qi S. Leonurine promotes the osteoblast differentiation of rat BMSCs by activation of Autophagy via the PI3K/Akt/mTOR pathway. *Front Bioeng Biotechnol.* 2021;9:615191. <https://doi.org/10.3389/fbioe.2021.615191>. PMID: 33708763.
  38. Dong J, Xu X, Zhang Q, Yuan Z, Tan B. The PI3K/AKT pathway promotes fracture healing through its crosstalk with Wnt/ $\beta$ -catenin. *Exp Cell Res.* 2020;394(1):112137. <https://doi.org/10.1016/j.yexcr.2020.112137>. PMID: 32534061.
  39. Song Y, Meng Z, Zhang S, Li N, Hu W, Li H. miR-4739/ITGA10/PI3K signaling regulates differentiation and apoptosis of osteoblast. *Regen Ther.* 2022;21:342–350. h32] Songdoi.org/<https://doi.org/10.1016/j.reth.2022.08.002>. PMID: 36161100.
  40. Yin R, Jiang J, Deng H, Wang Z, Gu R, Wang F. Mir-140-3p aggregates osteoporosis by targeting PTEN and activating PTEN/PI3K/AKT signaling pathway. *Hum Cell.* 2020;33(3):569–81. <https://doi.org/10.1007/s13577-020-00352-8>. PMID: 32253621.

## Publisher's note

Springer Nature remains neutral with regard to jurisdictional claims in published maps and institutional affiliations.